LETTER

Reversed flow of Atlantic deep water during the Last Glacial Maximum

César Negre[1], Rainer Zahn[1,2,3], Alexander L. Thomas[4], Pere Masqué[1,3], Gideon M. Henderson[4], Gema Martínez-Méndez[1]†, Ian R. Hall[5] & José L. Mas[6]

The meridional overturning circulation (MOC) of the Atlantic Ocean is considered to be one of the most important components of the climate system. This is because its warm surface currents, such as the Gulf Stream, redistribute huge amounts of energy from tropical to high latitudes and influence regional weather and climate patterns, whereas its lower limb ventilates the deep ocean and affects the storage of carbon in the abyss, away from the atmosphere. Despite its significance for future climate, the operation of the MOC under contrasting climates of the past remains controversial. Nutrient-based proxies[1,2] and recent model simulations[3] indicate that during the Last Glacial Maximum the convective activity in the North Atlantic Ocean was much weaker than at present. In contrast, rate-sensitive radiogenic $^{231}Pa/^{230}Th$ isotope ratios from the North Atlantic have been interpreted to indicate only minor changes in MOC strength[4–6]. Here we show that the basin-scale abyssal circulation of the Atlantic Ocean was probably reversed during the Last Glacial Maximum and was dominated by northward water flow from the Southern Ocean. These conclusions are based on new high-resolution data from the South Atlantic Ocean that establish the basin-scale north to south gradient in $^{231}Pa/^{230}Th$, and thus the direction of the deep ocean circulation. Our findings are consistent with nutrient-based proxies and argue that further analysis of $^{231}Pa/^{230}Th$ outside the North Atlantic basin will enhance our understanding of past ocean circulation, provided that spatial gradients are carefully considered. This broader perspective suggests that the modern pattern of the Atlantic MOC—with a prominent southerly flow of deep waters originating in the North Atlantic—arose only during the Holocene epoch.

A characteristic feature of our present ocean circulation is the deep convection that occurs in the North Atlantic and spreads North Atlantic Deep Water (NADW) to the world's abyssal oceans. This convection is compensated by the northward flow of warm subtropical surface waters that supply the North Atlantic with large amounts of heat. Changes in MOC therefore carry profound implications for global climate. Information about the operation of the MOC before the past 100 years is obtained from palaeoceanographic proxies, such as stable carbon isotopes ($\delta^{13}C$) and trace element ratios (Cd/Ca) recorded in the biogenic carbonate of bottom-dwelling foraminifera that trace the dispersal of biologically cycled nutrients in the ocean. Mapping of these palaeo-hydrographic data suggested that under glacial conditions nutrient-poor NADW ventilated a much smaller fraction of the deep Atlantic, which was dominated by Southern Component Waters (SCW) from the Southern Ocean[1,2,7]. This is consistent with deep-water temperature, salinity and oxygen reconstructions using independent proxy data and climate modelling[3,8]. These proxies, however, are influenced by deep water circulation and biological nutrient cycling alike, and do not allow a quantitative reconstruction of the abyssal flow rate, which sets marine heat transport and carbon storage.

Information on the abyssal flow rate of MOC can be deduced from the radiogenic isotope pair ^{231}Pa and ^{230}Th in sea-floor sediments[4,9,10]. This is due to their constant production in the water column from decay of dissolved uranium at a fixed $^{231}Pa/^{230}Th$ activity ratio of 0.093, and their differential solubility in the ocean (see Supplementary Information section 1 for details). Mapping of $^{231}Pa/^{230}Th$ ratios in Atlantic sea-floor sediments showed similar values in Last Glacial Maximum (LGM) and core-top sections, suggesting a southward transport of NADW during the LGM no different from, or possibly even stronger than, today[4]. Subsequent $^{231}Pa/^{230}Th$ records from the North Atlantic have indicated that measurable decreases in overturning occurred during millennial-timescale climate events in the deglaciation but indicate a still vigorous southward flow at the LGM[5,11–13]. This is in apparent conflict with the above-mentioned reconstructions derived from nutrient-based proxies[1,2,7].

Interpretation of $^{231}Pa/^{230}Th$ records in the North Atlantic to date assumes that the abundance of ^{231}Pa is solely modulated by the southerly flow of NADW, which should cause $^{231}Pa/^{230}Th$ in the South Atlantic to be higher than in the North Atlantic[10]. Critical assessment of this interpretation has hitherto been hindered by the lack of continuous fine-scale $^{231}Pa/^{230}Th$ records from the South Atlantic. Here we present such a record, measured at multi-centennial resolution in a sediment core recovered from the Cape basin (core MD02-2594; 34° 43′ S, 17° 20′ E). At a water depth of 2,440 m, the site is positioned in the present-day flow path of NADW, and its southerly position makes it particularly appropriate to reconstruct the strength of NADW relative to SCW. We measured a series of complementary proxies in MD02-2594 (Fig. 1): benthic $\delta^{18}O$ for stratigraphy; benthic $\delta^{13}C$ as an indicator of the nutrient content of ambient waters and chemical ventilation; sortable silt mean grain size ($\overline{SS}$) to assess near-bottom physical flow speed[14]; and opal concentrations for control on ^{231}Pa scavenging by variable biogenic silica fluxes[15,16]. Similar analyses were performed on cores further south to serve as reference for constraining $^{231}Pa/^{230}Th$ imprints of deep waters originating in the Southern Ocean (Supplementary Fig. 1).

The $^{231}Pa/^{230}Th$ ratios of core MD02-2594 display a pronounced increase from glacial values of 0.045 ± 0.005 (45–18 kyr before present, BP, $n = 15$, 1σ) to Holocene values of 0.065 ± 0.007 (10 kyr BP to present, $n = 15$). Such a shift is not observed in the associated data profiles of lithogenic sedimentation rate, authigenic U or opal flux, which argues against an imprint on the $^{231}Pa/^{230}Th$ profile by variable lithogenic flux or biological productivity. In fact, a prominent decrease is displayed by the total vertical particle flux going into the Holocene as $^{231}Pa/^{230}Th$ ratios increase. Therefore the $^{231}Pa/^{230}Th$ profile in this core primarily reflects ^{231}Pa variations driven by changes of deep Atlantic circulation. Benthic $\delta^{13}C$ and $\overline{SS}$ profiles from MD02-2594 display a clear glacial–interglacial shift, and support a major change in the basin-scale deep Atlantic circulation.

[1]Institut de Ciència i Tecnologia Ambientals (ICTA), Universitat Autònoma de Barcelona, 08193 Bellaterra, Spain. [2]Institució Catalana de Recerca i Estudis Avançats (ICREA), Lluís Companys 23, 08010 Barcelona, Spain. [3]Departament de Física, Universitat Autònoma de Barcelona, 08193 Bellaterra, Spain. [4]Department of Earth Sciences, University of Oxford, South Parks Road, Oxford OX1 3AN, UK. [5]School of Earth and Ocean Sciences, Cardiff University, Main Building, Park Place, Cardiff CF10 3YE, UK. [6]Dipartimento Física Aplicada I, Escuela Universitaria Politécnica, Universidad de Sevilla, Virgen de Africa 7, 41012 Sevilla, Spain. †Present address: Center for Marine Environmental Sciences (MARUM), University of Bremen, Leobener Strasse, 28359 Bremen, Germany.
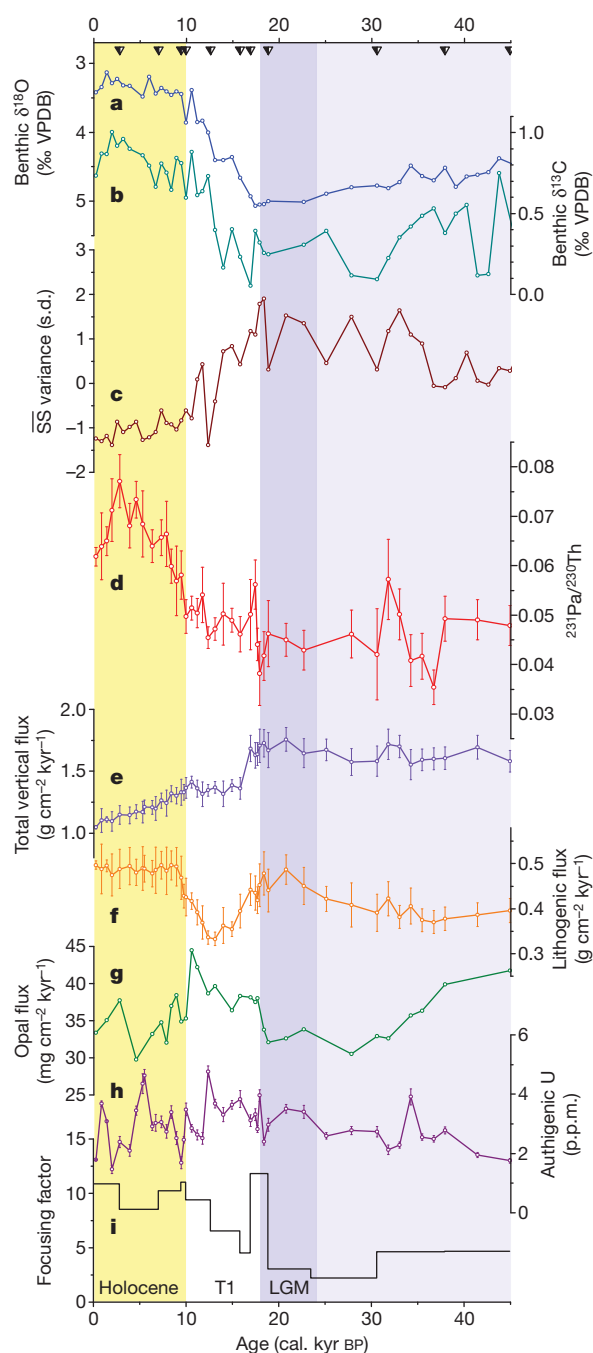
Figure 1 | Multi-proxy profiles of MD02-2594. a, b, Benthic stable isotope records of benthic foraminifera (*F. wuellerstorfi*) for $\delta^{18}O$ (**a**; left-hand *y* axis) and $\delta^{13}C$ (**b**; right-hand *y* axis). **c,** Sortable silt mean grain size ($\overline{SS}$) variance. **d,** $^{231}Pa/^{230}Th$. **e,** ^{230}Th-normalized total vertical particle flux. **f,** ^{230}Th-normalized lithogenic flux. **g,** ^{230}Th-normalized opal flux. **h,** Authigenic uranium concentration. The LGM to Holocene increase of sediment focusing (**i**) leads to lower exposure of core top sediments, less dissolution of opal and therefore less masking of real opal sedimentation, ruling out an influence of increased opal fluxes on $^{231}Pa/^{230}Th$ ratios. Triangles along upper *x*-axis mark ^{14}C ages. Error bars give analytical s.d. Vertical shading highlights Holocene (0–10 kyr BP), T1 (10–18 kyr BP) and LGM (18–24 kyr BP).

We assess the basin-scale abyssal flow by comparing our record with existing $^{231}Pa/^{230}Th$ profiles from North Atlantic sites (Fig. 2). For this we use a composite record of OCE326-GGC5 (33° 42′ N, 57° 35′ W, 4,550 m)[5] and SU90-44 (50° 01′ N, 17° 06′ W, 4,279 m)[13], which are positioned along the present NADW path upstream from MD02-2594. Comparison of late Holocene sections of the records (past 1.5 kyr) shows a $^{231}Pa/^{230}Th$ increase from the North Atlantic

(0.055 ± 0.002, *n* = 4) to the South Atlantic (0.064 ± 0.002, *n* = 3), reflecting ^{231}Pa advection with the southward flow of NADW. Applying a simple radiogenic isotope bottom water flow model[17] (see Methods), the late Holocene $^{231}Pa/^{230}Th$ gradient yields transit time estimates (TTEs) of 70 ± 30 yr for NADW to travel between 40° N and 35° S. These TTEs might be underestimated owing to resetting of the $^{231}Pa/^{230}Th$ signal by opal scavenging as waters pass the productive belt at the Equator, but recent work indicates that any such preferential Pa scavenging is minor in this setting during the late Holocene[18]. Indeed, the calculated TTE fits well with modern CFC-based observations[19].

At the LGM (24–18 kyr BP) the situation is fundamentally different and the $^{231}Pa/^{230}Th$ gradient between the South and North Atlantic is reversed. Core MD02-2594 displays $^{231}Pa/^{230}Th$ ratios substantially lower than those in equivalent sections of the North Atlantic records, resulting in a meridional $^{231}Pa/^{230}Th$ gradient that increases towards the north (see Supplementary Fig. 3 for additional data from the equatorial Atlantic[18]). The low values at MD02-2594 also contrast with high $^{231}Pa/^{230}Th$ ratios, well above the production ratio, in sediments from the Southern Ocean that reflect ^{231}Pa enrichment due to scavenging by biogenic opal[4,16,20]. Scavenging signals are also present in our companion record from the Agulhas Plateau that was close to, but not directly within, the northward-shifted opal belt of the LGM Southern Ocean (Supplementary Fig. 2).

The MD02-2594 $^{231}Pa/^{230}Th$ ratios hence reflect the presence of abyssal waters depleted in ^{231}Pa owing to opal scavenging[21], which leave the Southern Ocean to ventilate the deep Atlantic. Sedimentary $^{231}Pa/^{230}Th$ ratios at the LGM that are below production ratio at North Atlantic sites, previously interpreted to reflect vigorous flow from North Atlantic sources[4–6], are plausibly instead due to this northward flow of low-^{231}Pa waters. Our interpretation is consistent with indications derived from $\delta^{13}C$ and Cd/Ca that nutrient-rich bottom waters were present at deep core sites in the South and North Atlantic at the LGM[1,2,7]. Previous $^{231}Pa/^{230}Th$ interpretations did not consider the effect of ^{231}Pa scavenging in the Southern Ocean on the ^{231}Pa imprint of southern-sourced waters[4,5], and therefore overestimated deep ventilation from North Atlantic sources under full-glacial conditions. The meridional $^{231}Pa/^{230}Th$ gradient of ~0.03 at the LGM is somewhat larger than the (reverse) gradient seen during the Holocene, and suggests a flow from the Cape Basin to the North Atlantic at about half the rate seen in the opposite direction during the Holocene (Fig. 3). A reduced MOC vigour during the LGM is consistent with recent transient atmosphere–ocean model simulations[22], while increased seawater salinity (due to enhanced sea ice formation) stimulated deep water convection in the Southern Ocean hence promoting a flow from the south and driving the LGM abyssal flow reversal[3].

Along glacial Termination I (T1, 18–10 kyr BP), the South Atlantic $^{231}Pa/^{230}Th$ record displays a rather gradual increase that runs opposite to the North Atlantic profiles (Fig. 2). The only measurable step increase at our site is recorded immediately before the Heinrich 1 (H1) meltwater event in the North Atlantic. However, the coeval and more accentuated $^{231}Pa/^{230}Th$ shifts at the North Atlantic sites result in a steepened meridional gradient of 0.04 during H1. Although the $^{231}Pa/^{230}Th$ recorded in core OCE326-GGC5 during H1[5] may be compromised by enhanced biogenic opal deposition[23,24], $^{231}Pa/^{230}Th$ ratios in the subpolar North Atlantic likewise reached values close to the production ratio with low opal fluxes[12,13]. High ratios would thus reflect a weakening in the northward flow of the MOC, consistent with benthic $\delta^{13}C$, Cd/Ca and Nd isotope fingerprints in the subtropical North Atlantic that indicate the presence of waters from the south at this time[6,25]. During the Bølling–Allerød warm period (14.5–12.8 kyr BP), $^{231}Pa/^{230}Th$ and benthic $\delta^{13}C$ in MD02-2594 close to glacial levels still suggest a deep flow dominated by ^{231}Pa-depleted SCW. However, North and South Atlantic core sites at this time were bathed by different water masses owing to a restructuring of the Atlantic MOC[25], and hence the meridional $^{231}Pa/^{230}Th$ gradient in this period is not diagnostic of
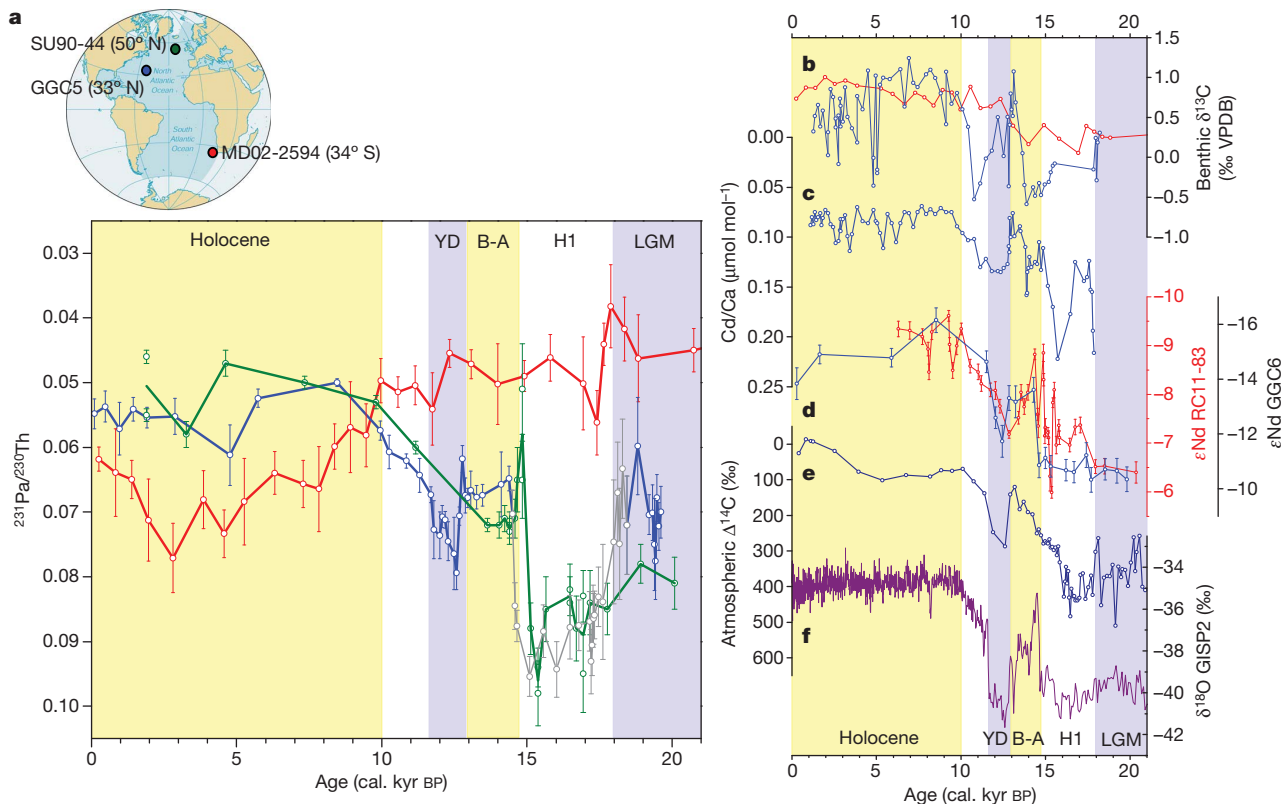
Figure 2 | MD02-2594 versus North Atlantic records. Atlantic proxy records depicting ocean circulation and climatic changes of the past 21 kyr. **a**, Top, core locations. Bottom, sedimentary $^{231}Pa/^{230}Th$ ratios from Cape Basin (MD02-2594; red; this study), eastern North Atlantic (SU90-44; green)[13] and Bermuda Rise (OCE326-GGC5; blue)[5]. The section 18.6–14.5 kyr BP of the OCE326-GGC5 record is influenced by opal scavenging[23] and is drawn in light grey. **b**, *F. wuellerstorfi* $\delta^{13}C$ measured in Cape Basin (MD02-2594; red; this study) and Bermuda Rise (EN120-GGC1, 33° 40′ N, 57° 37′ W, 4,450 m; blue)[25]

corrected for mean-ocean changes[29]. **c**, Benthic Cd/Ca from EN120-GGC1[25]; **d**, Nd isotope ratios (ε_{Nd}) in the Southeast Atlantic (RC11-83, 40° 36′ S, 9° 48′ E, 4,718 m; red)[27] and Bermuda Rise (OCE326-GGC6, 33° 41′ N, 57° 35′ W, 4,541 m; blue)[6]. **e**, Atmospheric $\Delta^{14}C$ profile from ODP Site 1002, Cariaco basin[28]. **f**, $\delta^{18}O$ record from GISP2, Greenland, indicating atmospheric temperature variations[30]. Error bars give analytical s.d. Vertical shading as Fig. 1, with Younger Dryas (YD; 11.5–12.8 kyr BP), Bølling–Allerød (B-A; 12.8–14.5 kyr BP) and H1 (~16.8 kyr BP).
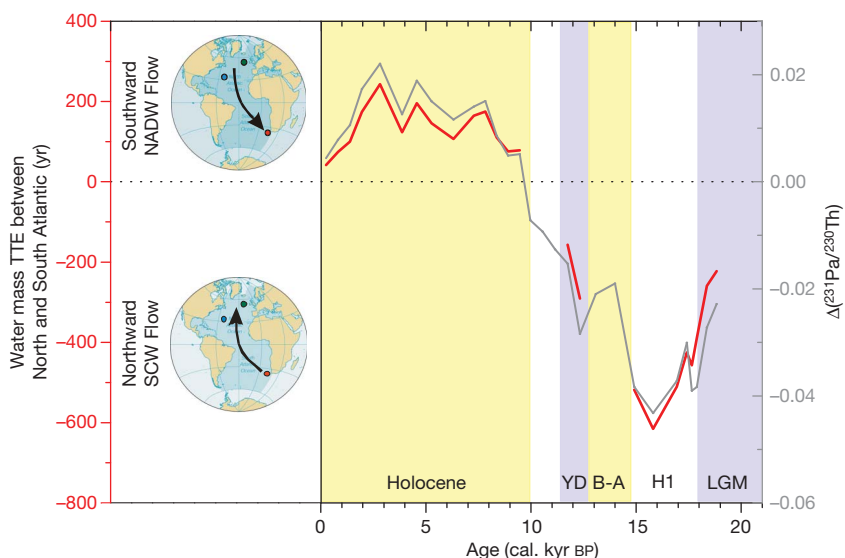

Figure 3 | Transit time estimates. Grey line (right *y*-axis), $^{231}Pa/^{230}Th$ gradient between MD02-2594 record and a composite of North Atlantic profiles SU90-44 and OCE326-GGC5. The composite (not shown) is an average of these two North Atlantic profiles (see Fig. 2), smoothed by a 5 point window and sampled at the time step of the MD02-2594 profile. The H1 interval in OCE326-GGC5 was excluded from the composite due to opal scavenging[23]. Red lines (left *y*-axis), transit time estimates (TTEs) between the

mid-latitude North Atlantic and the Cape Basin in the South Atlantic, computed with an isotope bottom water flow model[17]. TTE was computed only for periods when North and South Atlantic sites were bathed by the same water mass. Flow patterns (shown on maps; the upper map corresponds to the Holocene epoch; the lower map to YD, H1 and LGM time periods) are reversed during the LGM, indicating abyssal water flow from the South to the North Atlantic.

the basin-scale abyssal flow vigour. A resumption of SCW is indicated by nutrient proxy records in the subtropical North Atlantic during the subsequent Younger Dryas cold event (12.8–11.5 kyr BP). The meridional $^{231}Pa/^{230}Th$ distribution here suggests that the MOC dropped back to a mode and vigour similar to those at the LGM. The absence of any larger-scale deglacial $^{231}Pa/^{230}Th$ shifts in our profile suggests that transient episodes of changing convective activity at the sources of the northern water mass were not strong enough to allow the NADW flow to overcome SCW in the South Atlantic and affect $^{231}Pa/^{230}Th$ at the MD02-2594 site, confirming numerical tracer simulations[26].

Within 2 kyr of the end of the Younger Dryas episode, the $^{231}Pa/^{230}Th$ ratios from the North and South Atlantic converge. At ~9.7 kyr BP, the $^{231}Pa/^{230}Th$ gradient reverses, indicating the establishment of the modern flow pattern with vigorous basin-scale southward transport of NADW that causes ^{231}Pa enrichment in the South Atlantic relative to the North Atlantic. This is consistent with other proxy data, such as benthic Cd/Ca and $\delta^{13}C$ (ref. 25) as well as Nd isotopes[6,27], that all indicate enhanced ventilation by a nutrient-depleted well oxygenated water mass. Near-bottom physical flow speeds also reach interglacial levels at this time, as indicated by sedimentary $\overline{SS}$ in core MD02-2594 (Fig. 1), marking the retraction of SCW as the prominent source for deep ventilation of the South Atlantic. Atmospheric ^{14}C activities reach full interglacial levels[28], indicating that ancient carbon was completely flushed from the ocean abyssal carbon reservoir owing to the accelerated deep ventilation from North Atlantic sources. According to the $^{231}Pa/^{230}Th$ profiles, NADW advection to the south has remained an uninterrupted feature over the whole Holocene period (10–0 kyr BP) with average TTE of 130 ± 60 yr between 40° N and 35° S.

Our South Atlantic $^{231}Pa/^{230}Th$ profile has several implications. First, our data strongly suggest that the North Atlantic $^{231}Pa/^{230}Th$ ratios at the LGM reflect the flow of abyssal waters from the Southern Ocean to the north, rather than a southward flow from North Atlantic sources as suggested before[4,5]. Second, the LGM $^{231}Pa/^{230}Th$ gradient between our South Atlantic profile and published records from the North Atlantic is consistent with southern-sourced waters flowing northward at a rate about half the average southward-flowing NADW during the Holocene. This less vigorous deep flow is in agreement with recent numerical simulations[22]. Last, the absence of a $^{231}Pa/^{230}Th$ response in our profile to MOC perturbations forced by freshwater injection to the North Atlantic during the deglaciation supports tracer simulations[26] that demonstrate the insensitivity of our South Atlantic site to transient disruptions in the north. This therefore confirms that the progressive increase of $^{231}Pa/^{230}Th$ ratios seen in our profile from the LGM to the Holocene documents a longer-lasting reorganization of Atlantic circulation. It has previously been suggested that increased seawater salinity in the Southern Ocean[8] in combination with surface-ocean cooling at the LGM should have stimulated enhanced convective activity at southern sources, hence potentially favouring a reversed deep abyssal flow[3,22]. The prominent northward flow documented in the reversed $^{231}Pa/^{230}Th$ gradient at the LGM confirms these predictions and is relevant for understanding the sensitivity of the thermohaline circulation and for the calibration of climate models.

METHODS SUMMARY

For the determination of isotope abundances and $^{231}Pa/^{230}Th$, sediments were spiked and microwave-digested in a mixture of $HNO_3/HCl/HF$ and cleaned up with reverse aqua regia (Online Methods). Pa, Th and U were separated from each other using Dowex AG1-X8 resin, and measured with a Nu instruments multiple collector inductively coupled plasma mass spectrometer. The chronology of MD02-2594 was established with radiocarbon measurements of mono-specific planktonic foraminiferal samples. Analysis of $\delta^{18}O$ and $\delta^{13}C$ was performed on *Fontbotia wuellerstorfi* using a ThermoFinnigan MAT 252 mass spectrometer linked online to a single acid bath CarboKiel-II carbonate preparation device. $\overline{SS}$ measurements were undertaken on the terrigenous sub-fraction using a Coulter Multisizer III. Opal determination procedures followed extraction into Na_2CO_3, and quantification by the colorimetric heteropoly blue method. The

content of lithogenic material was computed from ^{232}Th; vertical rain rates of sedimentary constituents and focusing were estimated by ^{230}Th normalization.

Full Methods and any associated references are available in the online version of the paper at www.nature.com/nature.

1. Curry, W. B. & Oppo, D. W. Glacial water mass geometry and the distribution of $\delta^{13}C$ of ΣCO_2 in the western Atlantic Ocean. *Paleoceanography* **20,** PA1017, doi:10.1029/2004PA001021 (2005).
2. Marchitto, T. M. & Broecker, W. S. Deep water mass geometry in the glacial Atlantic ocean: a review of constraints from the paleonutrient proxy Cd/Ca. *Geochem. Geophys. Geosyst.* **7,** Q12003, doi:10.1029/2006GC001323 (2006).
3. Liu, Z., Shin, S., Webb, R. S., Lewis, W. & Otto-Bliesner, B. L. Atmospheric CO_2 forcing on glacial thermohaline circulation and climate. *Geophys. Res. Lett.* **32,** L02706, doi:10.1029/2004GL021929 (2005).
4. Yu, E. F., François, R. & Bacon, M. P. Similar rates of modern and last-glacial ocean thermohaline circulation inferred from radiochemical data. *Nature* **379,** 689–694 (1996).
5. McManus, J. F., Francois, R., Gherardi, J.-M., Keigwin, L. D. & Brown-Leger, S. Collapse and rapid resumption of Atlantic meridional circulation linked to deglacial climate changes. *Nature* **428,** 834–837 (2004).
6. Roberts, N. L., Piotrowski, A. M., McManus, J. F. & Keigwin, L. D. Synchronous deglacial overturning and water mass source changes. *Science* **327,** 75–78 (2010).
7. Lynch-Stieglitz, J. *et al.* Atlantic meridional overturning circulation during the Last Glacial Maximum. *Science* **316,** 66–69 (2007).
8. Adkins, J. F., McIntyre, K. & Schrag, D. P. The salinity, temperature, and $\delta^{18}O$ of the glacial deep ocean. *Science* **298,** 1769–1773 (2002).
9. Henderson, G. M. & Anderson, R. F. The U-series toolbox for paleoceanography. *Rev. Mineral. Geochem.* **52,** 493–531 (2003).
10. Marchal, O., Francois, R., Stocker, T. F. & Joos, F. Ocean thermohaline circulation and sedimentary $^{231}Pa/^{230}Th$ ratio. *Paleoceanography* **15,** 625–641 (2000).
11. Gherardi, J.-M. *et al.* Evidence from the Northeastern Atlantic basin for variability in the rate of the meridional overturning circulation through the last deglaciation. *Earth Planet. Sci. Lett.* **240,** 710–723 (2005).
12. Hall, I. R. *et al.* Accelerated drawdown of meridional overturning in the late-glacial Atlantic triggered by transient pre-H event freshwater perturbation. *Geophys. Res. Lett.* **33,** doi:10.1029/2006GL026239 (2006).
13. Gherardi, J.-M. *et al.* Glacial-interglacial circulation changes inferred from $^{231}Pa/^{230}Th$ sedimentary record in the North Atlantic region. *Paleoceanography* **24,** PA2204, doi:10.1029/2008PA001696 (2009).
14. McCave, I. N., Manighetti, B. & Robinson, S. G. Sortable silt and fine sediment size/composition slicing: parameters for paleocurrent speed and palaeoceanography. *Paleoceanography* **10,** 593–610 (1995).
15. Chase, Z., Anderson, R. F., Fleisher, M. Q. & Kubik, P. W. The influence of particle composition and particle flux on scavenging of Th, Pa and Be in the ocean. *Earth Planet. Sci. Lett.* **204,** 215–229 (2002).
16. Siddall, M. *et al.* $^{231}Pa/^{230}Th$ fractionation by ocean transport, biogenic particle flux and particle type. *Earth Planet. Sci. Lett.* **237,** 135–155 (2005).
17. Thomas, A. L., Henderson, G. M. & McCave, I. N. Constant bottom water flow into the Indian Ocean for the past 140 ka indicated by sediment $^{231}Pa/^{230}Th$ ratios. *Paleoceanography* **22,** PA4210, doi:10.1029/2007PA001415 (2007).
18. Bradtmiller, L. I., Anderson, R. F., Fleisher, M. Q. & Burckle, L. H. Opal burial in the equatorial Atlantic Ocean over the last 30 ka: implications for glacial-interglacial changes in the ocean silicon cycle. *Paleoceanography* **22,** PA4216, doi:10.1029/2007PA001443 (2007).
19. Huhn, O., Roether, W. & Steinfeldt, R. Age spectra in North Atlantic Deep Water along the South American continental slope, 10°N-30°S, based on tracer observations. *Deep Sea Res. I* **55,** 1252–1276 (2008).
20. Walter, H.-J., Rutgers van der Loeff, M. M. & Hoeltzen, H. Enhanced scavenging of ^{231}Pa relative to ^{230}Th in the South Atlantic south of the Polar Front: Implications for the use of the $^{231}Pa/^{230}Th$ ratio as a paleoproductivity proxy. *Earth Planet. Sci. Lett.* **149,** 85–100 (1997).
21. Thomas, A. L., Henderson, G. M. & Robinson, L. F. Interpretation of the $^{231}Pa/^{230}Th$ paleo circulation proxy: new water-column measurements from the southwest Indian Ocean. *Earth Planet. Sci. Lett.* **241,** 493–504 (2006).
22. Liu, Z. *et al.* Transient simulation of Last Deglaciation with a new mechanism for Bølling-Allerød warming. *Science* **325,** 310–314 (2009).
23. Keigwin, L. D. & Boyle, E. A. Did North Atlantic overturning halt 17,000 years ago? *Paleoceanography* **23,** PA1101, doi:10.1029/2007PA001500 (2008).
24. Lippold, J. *et al.* Does sedimentary $^{231}Pa/^{230}Th$ from the Bermuda Rise monitor past Atlantic meridional overturning circulation? *Geophys. Res. Lett.* **36,** L12601, doi:10.1029/2009GL038068 (2009).
25. Boyle, E. A. & Keigwin, L. D. North Atlantic thermohaline circulation during the past 20,000 years linked to high-latitude surface temperature. *Nature* **330,** 35–40 (1987).
26. Siddall, M. *et al.* Modeling the relationship between $^{231}Pa/^{230}Th$ distribution in North Atlantic sediment and Atlantic meridional overturning circulation. *Paleoceanography* **22,** PA2214, doi:10.1029/2006PA001358 (2007).
27. Piotrowski, A. M., Goldstein, S. L., Hemming, S. R. & Fairbanks, R. G. Temporal relationships of carbon cycling and ocean circulation. *Science* **307,** 1933–1938 (2005).
28. Hughen, K. A. *et al.* ^{14}C activity and global carbon cycle changes over the past 50,000 years. *Science* **303,** 202–207 (2004).
29. Zahn, R. & Stuber, A. Suborbital intermediate water variability inferred from paired benthic foraminiferal Cd/Ca and $\delta^{13}C$ in the tropical West Atlantic and linking with North Atlantic climates. *Earth Planet. Sci. Lett.* **200,** 191–205 (2002).

30. Grootes, P. M. Comparison of the oxygen isotope records from GISP2 and GRIP Greenland ice cores. *Nature* **366,** 552–554 (1993).

METHODS

Radiogenic isotope analysis. Determination of Pa, Th and U concentrations in sediments followed a recently published protocol[31]. Sediment (0.2 g) was spiked with ^{236}U, ^{229}Th and ^{233}Pa (milked from ^{237}Np; ref. 32), and microwave digested with a mixture of concentrated $HNO_3/HCl/HF$ (10:4:6 ml). Solutions were dried and 9 ml of reverse aqua regia (that is, HNO_3 and HCl mixed in a molar ratio of 3:1) added as an additional cleanup step. Fluorides were removed in three evaporation-dilution steps with HNO_3, and samples were finally dissolved in 4 ml HNO_3 7.5 M. Pa, Th and U were separated using Dowex AG1-X8 resin[33], pre-washed with HCl and Milli-Q water and preconditioned with 7.5 M HNO_3. Samples were loaded onto resin, washed with additional 4 ml of 7.5 M HNO_3, and the resin then converted to chloride form with 1.5 ml of 6 M HCl. Th, Pa and U were eluted with 6 ml of 6 M HCl, 6 M HCl + 0.05 M HF, and Milli-Q water, respectively; the Pa fraction was further purified with a repeat anion-exchange separation. Isotope abundances (^{230}Th, ^{231}Pa, ^{232}Th, ^{238}U) were measured on a Nu Instruments MC-ICPMS at Oxford University following standard protocols[21]. In-run uncertainties (1σ) of single measurements were <2% for all isotopes. For Th and U, around 90% of the uncertainties originated from the calibration of the ^{229}Th and ^{236}U tracers used in this study. Reproducibility (including possible sample heterogeneity) is 7.0% for ^{231}Pa, 1.6% for ^{230}Th, 4.6% for ^{232}Th and 2.7% for ^{238}U.

Excess sedimentary ^{231}Pa and ^{230}Th activities were calculated correcting total concentrations for detrital and authigenic components (details in Supplementary Information section 4). Terrigenous material concentrations were inferred from ^{232}Th, assuming a ^{232}Th concentration of 10.7 p.p.m. in lithogenic material[34]. Vertical rain rates of sedimentary constituents and sediment focusing were estimated by ^{230}Th normalization[35].

Chronology. The chronology of core MD02-2594 is based on 11 accelerator mass spectrometry (AMS) radiocarbon measurements[36]. The analyses were performed on mono-specific planktonic foraminiferal samples (*Globorotalia inflata*) containing more than 3 mg of carbonate. Sample preparation and ^{14}C measurements were carried out at the National Ocean Sciences Accelerator Mass Spectrometry Facility (NOSAMS) at Woods Hole Oceanographic Institution. Radiocarbon ages were corrected applying a reservoir age of 615 ± 52 yr (ref. 37) and converted to calendar years (ref. 38).

The one-dimensional $^{231}Pa/^{230}Th$ model. Deep water TTEs were computed by importing sedimentary $^{231}Pa/^{230}Th$ ratios into a 1D model[17]. The model is a simplified representation of the processes that influence ^{231}Pa and ^{230}Th scavenging during water mass transit. The ocean is divided into 500-m-deep boxes down to 4,000 m water depth. Production of particles settling through the underlying boxes is determined in the surface box with typical open-ocean carbonate particle flux of $0.06\ g\ m^{-2}\ d^{-1}$ (ref. 39); distribution coefficients for Pa and Th between particulate and dissolved fractions (K_d) are taken from refs 15 and 16.

Stable isotopes ($\delta^{18}O$ and $\delta^{13}C$). Benthic $\delta^{18}O$ and $\delta^{13}C$ analyses followed standard protocols[40]. Sediment samples were freeze-dried to facilitate desegregation and to minimize physical damage on microfossils during wet sieving. Samples were sieved over a 63-μm screen to separate sediment coarse and fine fractions. The fine fraction (<63 μm) was oven-dried at 50 °C, weighed and used for $\overline{SS}$ analyses (see below). The coarse fraction was used for foraminiferal separation. Between 3 and 7 specimens of the epibenthic foraminifera *F. wuellerstorfi* were picked from the size fraction 250–315 μm at 10-cm steps. Cleaning procedures before stable isotope analysis involved light mechanical crushing under methanol followed by ultrasonication for 10–20 s to remove sediment coatings and release possible sediment infill. Stable isotopes were measured with a ThermoFinnigan MAT 252 mass spectrometer linked online to a single acid bath CarboKiel-II carbonate preparation device at Cardiff University. External reproducibility was monitored with an internal laboratory standard (Solenhofen Limestone) and was 0.07‰ for $\delta^{18}O$ and 0.03‰ for $\delta^{13}C$. All isotope values are referred to the Vienna Peedee Belemnite scale (VPDB) through calibration to the NBS-19 carbonate standard. Benthic $\delta^{18}O$ values are presented on the *Uvigerina* scale by adding 0.64‰ to each *F. wuellerstorfi* measurement to accommodate isotope offsets of this species from oxygen isotope equilibrium with ambient sea water[41]. Benthic $\delta^{13}C$ values were corrected for mean-ocean changes[29].

Sortable silt analysis. Before $\overline{SS}$ analysis, carbonate and biogenic opal were removed from the fine fraction by dissolution in 1 M acetic acid (48 h at room temperature) and digestion in 2 M Na_2CO_3 (85 °C for 5 h), respectively. The $\overline{SS}$ grain size measurements were undertaken on the residual terrigenous sub-fraction using a Coulter Multisizer III[42]. The analytical precision ranges between 1 and 4%.

Biogenic opal analysis. Opal digestion was carried out following ref. 43. 5 ml of 10% H_2O_2 was added to 50 mg of sample in order to break down organic matter; after 30 min, an additional 5 ml of 1 M HCl were added to dissolve carbonates. Samples were sonicated for 30 min and after another 30 min, 20 ml of Milli-Q water was added and containers centrifuged at 4,500 r.p.m. for 6 min. Containers were then decanted to discard the supernatant and placed in an oven overnight at 60 °C to remove moisture. 40 ml of 2 M Na_2CO_3 were added to each sample, which were shaken and sonified, and placed in a constant-temperature bath at 85 °C to dissolve silica. After 2 and 4 h containers were shaken and placed in the bath, and after 5 h centrifuged for 6 min at 4,500 r.p.m. The supernatant was stored for analysis.

Opal analysis was performed using the colorimetric heteropoly blue method[44]. 9.5 ml of Milli-Q water were added to clean polypropylene tubes, together with 0.2 ml of molybdate reagent. After 10 min, 0.2 ml of citric acid and 0.2 ml of amino-naphthol sulphonic acid were added and left for another 10 min. Next, 0.1 ml of sample solution was added to each tube and left to react for one hour. Solutions were then transferred to spectrophotometer cells and measured with a Hach Lange DR2800 spectrophotometer. A blank bracketed every sample and a standard solution was measured to monitor machine drift. Method reproducibility was ~10%.

31. Negre, C. *et al.* Separation and measurement of Pa, Th, and U isotopes in marine sediments by microwave-assisted digestion and multiple collector inductively coupled plasma mass spectrometry. *Anal. Chem.* **81,** 1914–1919 (2009).
32. Regelous, M., Turner, S. P., Elliott, T. R., Rostami, K. & Hawkesworth, C. J. Measurement of femtogram quantities of protactinium in silicate rock samples by multicollector inductively coupled plasma mass spectrometry. *Anal. Chem.* **76,** 3584–3589 (2004).
33. Edwards, R. L., Chen, J. H. & Wasserburg, G. J. ^{238}U-^{234}U ^{230}Th-^{232}Th systematics and the precise measurement of time over the past 500,000 years. *Earth Planet. Sci. Lett.* **81,** 175–192 (1986).
34. Taylor, S. R. & McLennan, S. M. *The Continental Crust: its Composition and Evolution* (Blackwell, 1985).
35. François, R., Frank, M., Rutgers van der Loeff, M. M. & Bacon, M. P. ^{230}Th normalisation: an essential tool for interpreting sedimentary fluxes during the late Quaternary. *Paleoceanography* **19,** PA1018, doi:10.1029/2003PA000939 (2004).
36. Martínez-Méndez, G. *et al.* Contrasting multi-proxy reconstructions of surface ocean hydrography in the Agulhas Corridor and implications for the Agulhas Leakage during the last 345,000 years. *Paleoceanography* doi:10.1029/2009PA001879 (in the press).
37. Southon, J., Kashgarian, M., Fortugne, M., Metivier, B. & Yim, W. E.-S. Marine reservoir corrections for the Indian Ocean and Southeast Asia. *Radiocarbon* **44,** 167–180 (2002).
38. Fairbanks, R. G. *et al.* Radiocarbon calibration curve spanning 0 to 50,000 years BP based on paired $^{230}Th/^{234}U/^{238}U$ and ^{14}C dates on pristine corals. *Quat. Sci. Rev.* **24,** 1781–1796 (2005).
39. Honjo, S. & Manganini, S. J. Annual biogenic particle fluxes to the interior of the North Atlantic Ocean: studied at 34° N 21° W and 48° N 21° W. *Deep Sea Res. II* **40,** 587–607 (1993).
40. Martínez-Méndez, G., Zahn, R., Hall, I. R., Pena, L. D. & Cacho, I. 345,000-year long multi-proxy records off South Africa document variable contributions of northern versus southern component water to the deep South Atlantic. *Earth Planet. Sci. Lett.* **267,** 309–321 (2008).
41. Shackleton, N. J. Attainment of isotopic equilibrium between ocean water and the benthonic foraminifera genus Uvigerina: isotopic changes in the ocean during the last glacial. *Colloq. Int. CNRS* **219,** 203–209 (1974).
42. Bianchi, G. G., Hall, I. R., McCave, I. N. & Joseph, L. Measurements of the sortable silt current speed proxy using the Sedigraph 5100 and Coulter Multisizer IIe: precision and accuracy. *Sedimentology* **46,** 1001–1014 (1999).
43. Mortlock, R. A. & Froelich, P. N. A simple method for the rapid determination of biogenic opal in pelagic marine sediments. *Deep-Sea Res.* **36,** 1415–1426 (1989).
44. Koroleff, F. in *Methods of Seawater Analysis* 2nd edn (eds Grasshoff, K., Kremling, K. & Ehrhardt, M.) 174–183 (Verlag Chemie, Weinheim, 1983).